Supporting information

Organic-Inorganic Hybrid Co-Containing Polyoxotungstates as Oxygen Evolution Catalyst

Zhe-Hong Chen,[†] Xiao-Yue Zhang,[†] Da-Huan Li, Xin-Xiong Li, Yan-Qiong Sun, Cai Sun[*] and Shou-Tian Zheng[*]

Fujian Provincial Key Laboratory of Advanced Inorganic Oxygenated Materials, College of Chemistry, Fuzhou University, Fuzhou, Fujian 350108, China.

China. E-mail: csun@fzu.edu.cn(C. Sun); stzheng@fzu.edu.cn (S.-T. Zheng).

Index

Experimental section

Materials and measurements. Except that the $K_8Na_2[GeW_9O_{34}]\cdot 25H_2O$ precursors were synthesized according to a method reported in the literature, all chemicals used for syntheses were purchased from commercial sources, and no further purifications were conducted before their usages. EInfrared (IR) spectra (KBr pellet) was performed on an Opus Vetex 70 FTIR infrared spectrophotometer in the range of 400-4000 cm^{-1}. Powder X-ray diffraction (PXRD) patterns were recorded on a Rigaku DMAX 2500 diffractometer with MoKα radiation (λ = 0.71073 Å). Thermogravimetric analysis was conducted using a Mettler Toledo TGA/SDTA 851^e analyzer in an N_2-flow atmosphere with a heating rate of 10 °C/min at a temperature of 25-800 °C. The UV-vis spectrum was measured on a SHIMADZU UV-2600 UV-visible spectrophotometer. Simulated XRD data was simulated by the Mercury Software with the step of 0.02° from 5° to 50° (λ = 0.71073 Å).

Synthesis of $H_2K_4[Co(H_2O)_6][Co(bpdo)(H_2O)_5]_2\ [Co_4(H_2O)_2(B\text{-}\alpha\text{-}GeW_9O_{34})_2]\cdot 3bpdo\cdot 16H_2O$ (Co-POW)

A mixture of $K_8Na_2[GeW_9O_{34}]\cdot 25H_2O$ (0.150 g, 0.049 mmol), $Co(Ac)_2\cdot 4H_2O$ (0.045 g, 0.181mmol), bpdo (0.039 g, 0.207 mmol), were mixed in 5 mL deionized water and 3 mL pH 4.5 buffer solution (HAc/NaAc) in a 20 mL glass bottle. After stirred for 1 hour, the resulting mixture was heated at 100 °C for 72 h. After cooling down to room temperature, the resulting solution was filtered and kept at room temperature for slow evaporation, red crystals were obtained. Yield: 20 mg (12.3 %, based on W).

Synthesis of $H_2K_4[Zn(H_2O)_6][Zn(bpdo)(H_2O)_5]_2\ [Zn_4(H_2O)_2(B\text{-}\alpha\text{-}GeW_9O_{34})_2]\cdot 3bpdo\cdot 16H_2O$ (Zn-POW)

A mixture of $K_8Na_2[GeW_9O_{34}]\cdot 25H_2O$ (0.150 g, 0.049 mmol), $ZnCl_2$ (0.035 g, 0.257 mmol) , bpdo (0.039 g, 0.207 mmol), were mixed in 5 mL deionized water and 3mL pH 4.5 buffer solution (HAc/NaAc) in a 20 mL glass bottle. After stirred for 1 hour, the resulting mixture was heated at 100 °C for 72 h. After cooling down to room temperature, the resulting solution was filtered and kept at room temperature for slow evaporation, colorless crystals were obtained. Yield: 17 mg (10.5 %, based on W).

X-ray crystallographic study: Single-crystal X-ray diffraction measurements were performed on a D8 Quest, using graphite monochromated Mo K_α radiation (λ = 0.71073 Å). Intensity data sets were collected using ω scan techniques and corrected for *Lp* effects. The structures were solved by the direct method and refined by full-matrix least squares on F^2 using the Siemens SHELXTL^{TM} Version 5 package of crystallographic software with anisotropic thermal parameters for all non-hydrogen atoms. Hydrogen atoms were added geometrically and refined using the riding model. Crystal data and structure refinement results for **1** are summarized in Table S2.

The entries of CCDC-2355472 and 2355473 contain the supplementary crystallographic data for **Co-POW** and **Zn-POW**. These data can be obtained free of charge at http://www.ccdc.cam.ac.uk/conts/retrieving.html or from the Cambridge Crystallographic Data Centre, 12, Union Road, Cambridge CB2 1EZ, U.K. Fax: (Internet) +44-1223/336-033. E-mail: depos-it@ccdc.cam.ac.uk.

The preparation of the working electrode. For the preparation of the working electrode, 5 mg of catalyst was dispersed in a mixed solution containing 120 µL of isopropyl alcohol and 370 µL of 5 vol% aqueous Nafion. Then, the suspension was ultrasonicated for 30 minutes to form a homogeneous ink. The carbon cloth (CC) was first degreased by sonication in acetone and carefully washed with 0.5 M HCl in an ultrasonic bath for 20 min to remove the surface oxidation layer. Finally, apply 60 µL of catalyst ink in a uniform drop onto a CC with an area of 1 × 1 cm^2 and controlled catalyst loading of 0.5 mg cm^{-2}.

Electrochemical OER Measurements: The electrochemical performance was tested on a three-electrode electrochemical workstation (Zennium-pro, Germany Zahner Instrument) fabricated from a working electrode, a graphite counter electrode, and an Ag/AgCl reference electrode (in 1 M KCl). The test electrolyte is 0.1 M phosphate buffer solution (PBS, pH = 7.4) and normalized concerning the reversible hydrogen electrode (RHE)

according to Equation: $E_{vs.RHE} = E_{vs.Ag/AgCl} + 0.0591 \times pH + 0.222$ V. All potentials have been converted to RHE without specific indication. The OER polarization curve was obtained using linear scanning voltammetry at a scan rate of 5 mV s^{-1} over a potential range of 1.2 to 2.2 V, and correction of the stable current issue by 91% iR compensation. The contribution of the blank CC lectrode to the OER current was negligible (Figure S7). The Tafel slopes were calculated from the linear region of the LSV polarization curve according to the equation: $\eta = b \times \log j + a$, in which η is the overpotential, b is the Tafel slope, and j is the current density. To evaluate the charge transfer resistance, the EIS was performed at open circuit potential (1.60 V) with an AC voltage amplitude of 5 mV and a frequency of 0.1 Hz to 100 KHz. The electrochemical double-layer capacitance (C_{dl}) was estimated by CV scans in a non-Faradic region at various scan rates from 20 to 120 mV s^{-1}. The C_{dl} values were estimated by plotting $\Delta j = (j_a - j_c)$ at 0.975 V against the scan rates. Whereby, j_a and j_c are the anode and cathode current densities, respectively. All experiments were performed at room temperature (25 ± 1 °C).

Supplementary Tables.

Table S1. Comparison of OER performances of the electrocatalysts in neutral electrolytes.

Catalyst	Electrolyte	Overpotential (mV)	Current density (mA cm^{-2})	Reference
Ultrathin Co_3S_4 nanosheets	0.1 M PBS (pH = 7.0)	620	3	3
$Co(PO_3)_2$ nanoparticles	0.1 M PBS (pH = 6.4)	590	10	5
Co_3O_4 nanorods	0.1 M Na_2SO_4 (pH = 7.0)	606	1	7
bulk Co_3S_4	0.1 M PBS (pH = 7.0)	690	0.3	3
Co_3S_4/ TETA	0.1 M PBS (pH = 7.0)	580	0.12	3
CoPi / N-graphene	0.1 M PBS (pH = 7.0)	~ 200	1	2
Co-Pi nanoarray/Ti	0.1 M PBS (pH = 7.0)	460	10	4
Co_3O_4/SWNTs	0.1 M PBS (pH = 7.0)	400	1	6
Co-POM	0.1 M PBS (pH = 7.4)	515	10	This Work

Table S2. Crystallographic data for **Co-POW** and **Zn-POW**.

	Co-POW	**Zn-POW**
Formula	$C_{25}H_{40}Co_{3.5}GeK_2N_5O_{54}W_9$	$C_{25}H_{40}Zn_{3.5}GeK_2N_5O_{54}W_9$
Mr	3286.31	3303.37
Crystal size (mm^3)	0.2 × 1 × 1.5	0.2 × 1.4 × 2.4
Crystal system	Triclinic	Triclinic
Space group	$P\bar{1}$	$P\bar{1}$
a/Å	11.7657(3)	11.7109(3)
b/Å	15.6126(3)	15.5844(6)
c/Å	19.2536(4)	19.2261(8)
α/°	67.274(2)	67.382(4)
β/°	76.636(2)	76.551(3)
γ/°	87.587(2)	87.841(2)
V/Å^3	3169.45(13)	3145.0(2)
Z	2	2
ρ_{calc} g/cm^3	3.444	3.488
μ/mm^{-1}	17.863	18.413
F(000)	2975.0	2993.0
Radiation	MoK_α (λ = 0.71073)	MoK_α (λ = 0.71073)
Reflections collected	32809	31183
Independent reflections	11136 [R_{int} = 0.0361, R_{sigma} = 0.0445]	11072 [R_{int} = 0.0614, R_{sigma} = 0.06]
Data/restraints/parameters	11136/78/984	11072/169/930
GOF on F^2	1.064	1.070
Final R indexes [I≥2σ (I)]	R_1 = 0.0526, wR_2 = 0.1436	R_1 = 0.0620, wR_2 = 0.1792
Final R indexes [all data]	R_1 = 0.0744, wR_2 = 0.1605	R_1 = 0.0875, wR_2 = 0.2039
Data completeness	0.958	0.958

$R_1{}^a = \sum||F_o| - |F_c||/\sum|F_o|$. $wR_2 = [\sum w(F_o^2 - F_c^2)^2/\sum w(F_o^2)^2]^{1/2}$

Table S3. BVS calculations of all the Co atoms for **Co-POW**.

Atoms	Calcd for Co^{II}	Oxidation state
Co1	2.11	Co^{II}
Co2	2.09	Co^{II}
Co3	2.03	Co^{II}
Co4	2.21	Co^{II}

Table S4. Fitted data of the electrochemical impedance spectroscopy analysis.

samples	R_0/Ω	CPE_1/mF	R_1/Ω	CPE_2/μF	R_2/Ω	Overall Error
Zn-POW	1.05	20.1	22.5	68.3	1.02	0.47%
Co-POW	1.12	7.09	75.2	17.1	1.24	0.83%

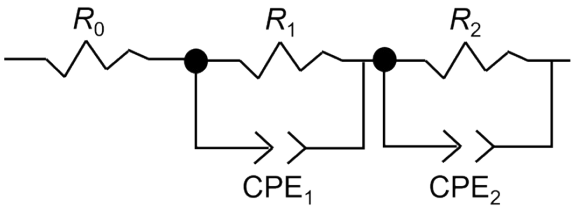

The equivalent circuit is used in fitting the plot.

R_0: solution resistance; R_1 or R_2: charge transfer resistance; CPE_1 or CPE_2: constant phase element. The two *R*-CPE units represent two electransfer processes. One is the electrochemical oxidation of H_2O by electron transfer at the liquid-solid interface. The other is the transfer of electrons to a carbon cloth electrode via a catalyst. The former was a more sluggish process than the latter. Therefore, a larger charge transfer resistance (R_1) corresponds to the electrochemical charge transfer process.

Supplementary Figures.

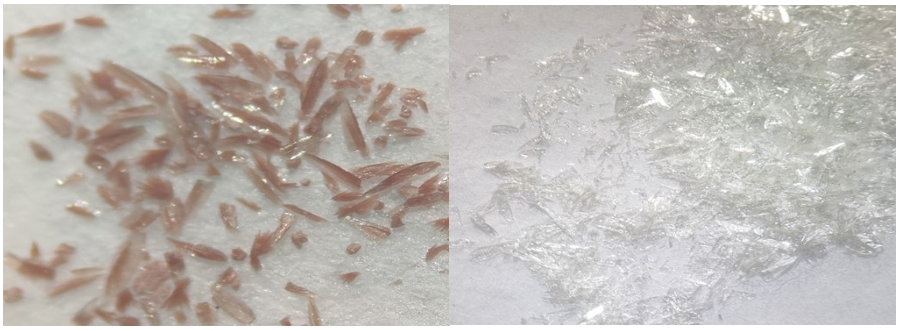

Fig. S1. Crystal morphology of **Co-POW** (left) and **Zn-POW** (right).

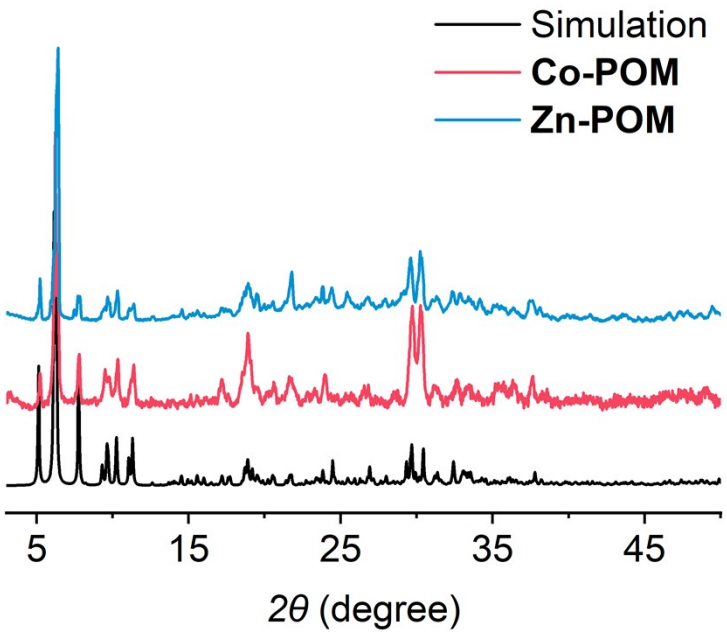

Fig. S2. The simulated and experimented powder XRD patterns for **Co-POW** and **Zn-POW**.

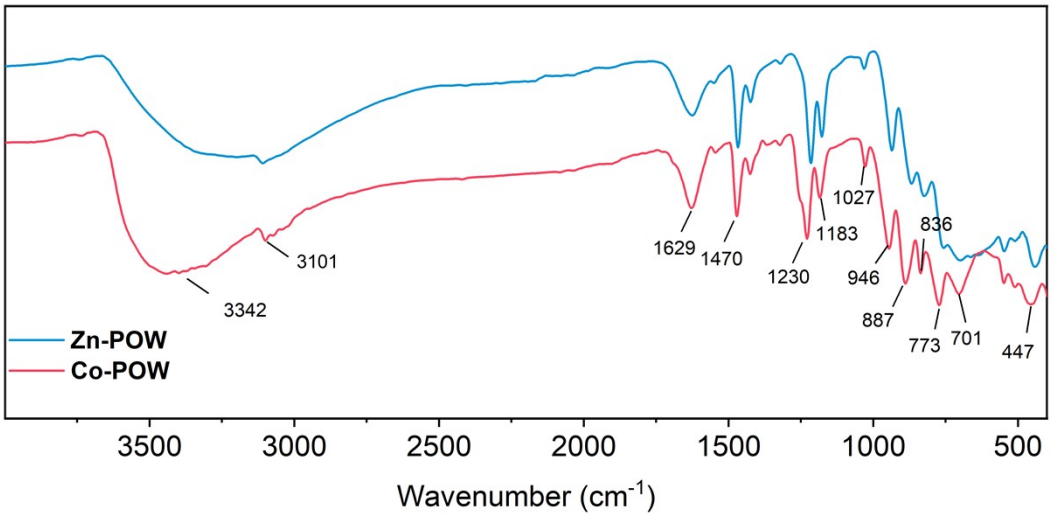

Fig. S3. IR curves of **Co-POW** and **Zn-POW**.

The IR spectrum of **Zn-POW** is similar to **Co-POW**. Peaks at 3101 cm^{-1} ascribe to the *v*(=C-H); peaks at 1629, 1470 cm^{-1} ascribe to the *v*(pyridine skeleton); peaks at positions 1350-1100 cm^{-1} mainly ascribe to the *v*(C-N); the peaks below 1000 cm^{-1} mainly ascribe to the *v*(W-O), and partly *δ*(=C-H); the peak at 3342 cm^{-1} derived from *v*(O-H) of H_2O.

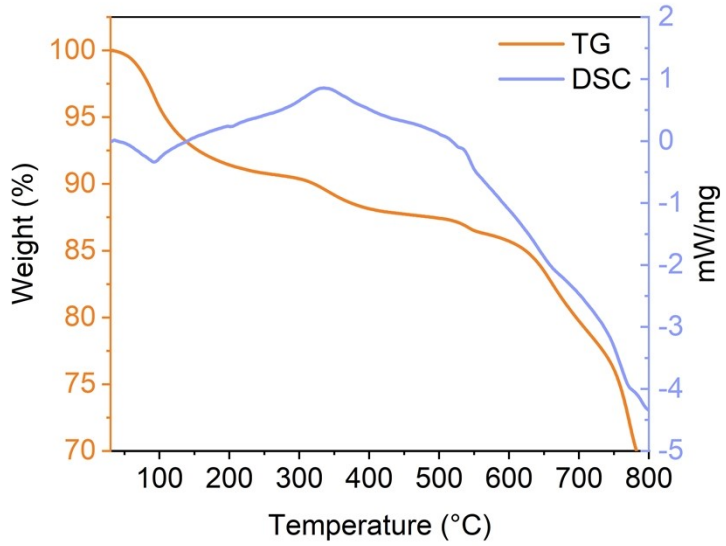

Fig. S4. TGA curve for **Co-POW**.

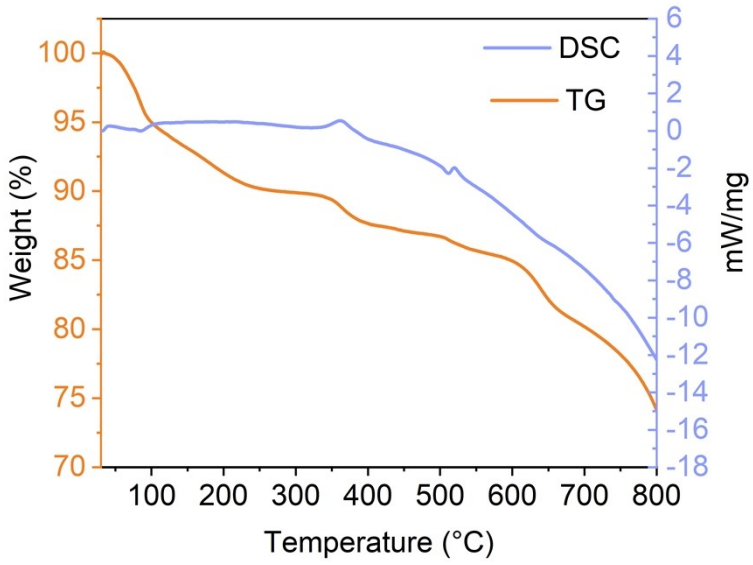

Fig. S5. TGA curve for **Zn-POW**.

The thermogravimetric curve of **Co-POW** was measured at a heating rate of 10 °C/min in a N_2-flow atmosphere, and the temperature range of the test was from 25 °C to 800 °C. The TGA curve of **Co-POW** is similar with the one of **Zn-POW**. As shown in Fig.S4, **Co-POW** has a continuous weight loss process in the temperature range of 25 °C to 800 °C. The first weight-loss stage within the range of 25 °C to 220 °C mainly ascribed to the loss of water molecules. Based on the first weight-loss of about 9.3 % for **Co-POW**, there are about 34 water molecules.

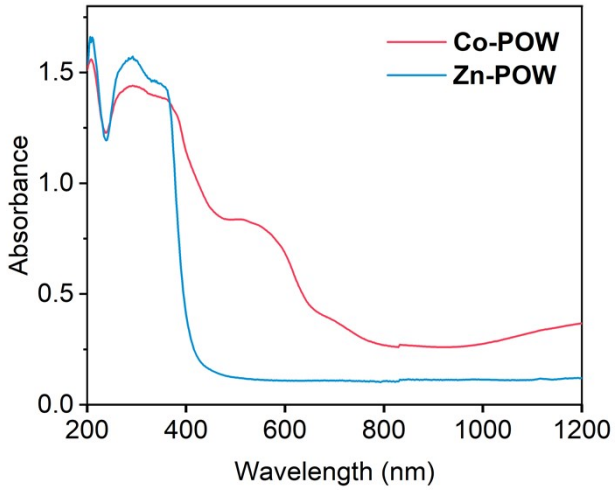

Fig. S6. UV-Vis absorption spectra of **Co-POW** and **Zn-POW**.

The UV-Vis absorption spectra of compounds are determined in the range of 200 to 1200 nm. The absorption peak in the range of 200 to 400 nm can be attributed to the charge transfer transitions from O to W. The broad absorption peak in the range of 400 to 600 nm can be attributed to the d-d transition of the 3d transition metal Co^{II}.

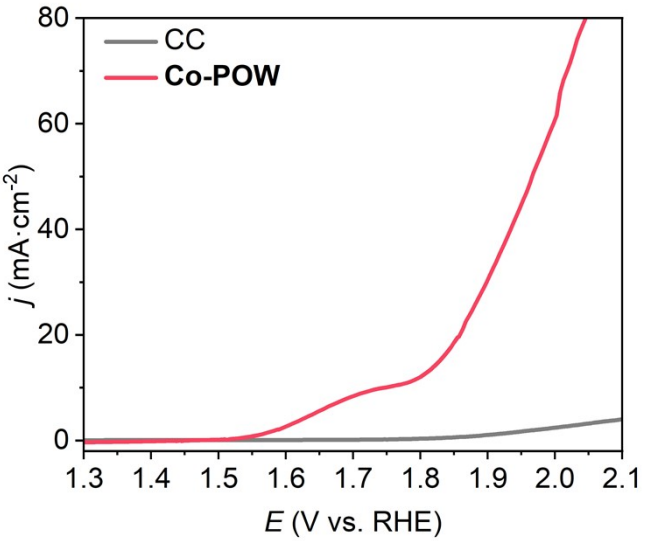

Fig. S7. Comparison of the Electrochemical activity of **Co-POW** and CC.

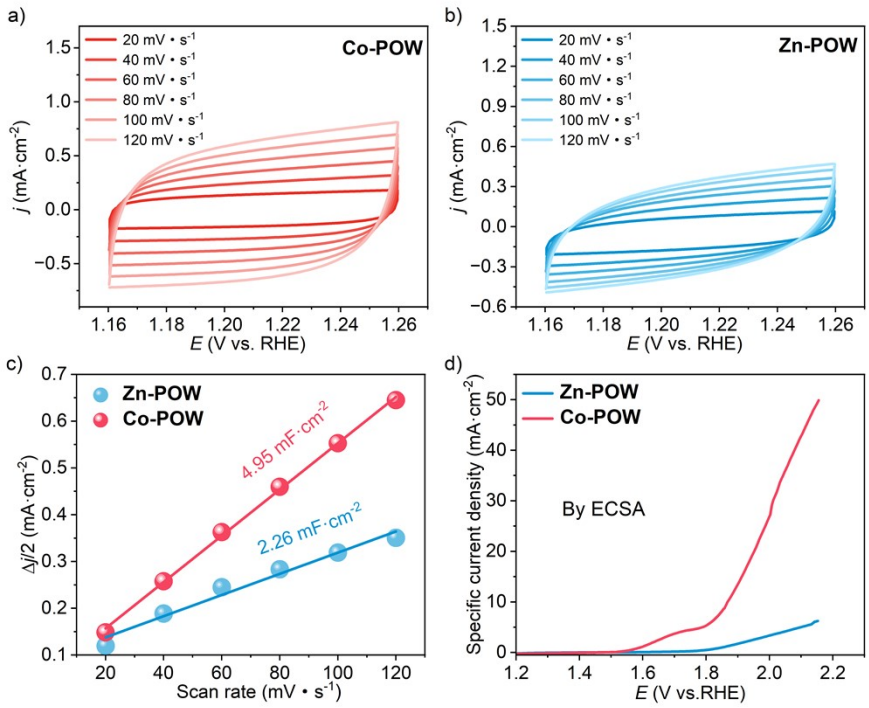

Fig. S8. Measurement of C_{dl}.

CV cycles for **Co-POW** (a) and **Zn-POW** (b) at different scan rates increasing from 20 to 120 mV s^{-1}. (f) C_{dl} of catalysts derived from current density versus the scan rate. With the measurement of the electrochemical double layer capacitance (C_{dl}) of the prepared electrocatalysts, the electrochemically active surface area (ECSA) of the samples was further estimated. As expected, the **Co-POW** catalyst possesses more available active sites with a C_{dl} value of 4.95 mF cm^{-2}, which is higher than those of **Zn-POW** (2.26 mF cm^{-2}). To eliminate the impact of different mass loadings of the catalyst on the carbon cloth surface, the current density was normalized against the electrochemical active surface area (ECSA) (Fig. S7d). This also shows that **Co-POW** has relatively higher intrinsic oxygen evolution reaction activity compared to **Zn-POW**, which is in agreement with the above data.

3. References

1. G. M. Sheldrick, *Acta Cryst.*, **2008**, *A64*, 112-122.
2. A. Vasileff , S. Chen and S. Z. Qiao, *Nanoscale Horiz*, ***2016***, *1*, 41–44.
3. Y. Liu, C. Xiao, M. Lyu, Y. Lin, W. Cai, P.Huang, W. Tong, Y. Zou and Y. Xie, *Angew Chem Int Ed*., **2015**, *54*, 11231–11235.
4. L. Cui, D. Liu, S. Hao, F. Qu, G. Du, J. Liu, A. M. Asiri and X. Sun, *Nanoscale.* **2017**, *9*, 3752–3756.
5. HS. Ahn and TD. Tilley, *Adv Funct Mater.* **2013**, *23*, 227–233.
6. J. Wu, Y. Xue, X. Yan, W. Yan, Q. Cheng and Y. Xie, *Nano Res.* **2012**, *5*, 521–530.